Analysis of ^1H and ^{13}C Nuclear Magnetic Resonance Spectra of Spathulenol by Two-dimensional Methods

Fuyihiko Inagaki* and Akira Abe
Toray Research Center Inc., 1111, Tebiro, Kamakura, 248 Japan

Several two-dimensional n.m.r. (2D-n.m.r.) methods have been used for the structural analysis of spathulenol, a sesquiterpene alcohol from the peel oil of *Citrus junos* Tanaka. First, ^{13}C resonances were classified into those due to CH, CH_2, CH_3, and quaternary carbon by INEPT. Next, ^1H–^{13}C shift-correlated 2D-n.m.r. was used to assign the pairs of directly bonded ^1H and ^{13}C nuclei. Finally, ^1H shift-correlated 2D-n.m.r. was employed to study the network of spin couplings in the molecule. From these data, the skeletal structure of spathulenol was determined. Finally, n.O.e.-correlated 2D-n.m.r. and the n.O.e. difference method were applied to determine the three-dimensional structure of spathulenol and to achieve complete assignment of ^1H and ^{13}C resonances.

The availability of two-dimensional n.m.r. (2D-n.m.r.) opens a new era for the structure determination of organic molecules. The ability to develop chemical shifts (and coupling constants) into two dimensions, and to resolve overlap of resonances, enables the correlation of interacting nuclei to be determined unambiguously. As a result of its high resolving power, 2D-n.m.r. can be applied to complex spectra which are difficult and time consuming to analyse by conventional methods. Several reported 2D-n.m.r. methods are useful for the structure determination of organic molecules.[1–4] In particular, INADEQUATE 2D-n.m.r. is an elegant method for determining skeletal structures.[5–7] However, owing to its low sensitivity, this method cannot be applied in practice to small quantities, such as samples of naturally occurring substances. In the present study, we propose a practical approach to the structure analysis of naturally occurring substances by 2D-n.m.r., which we have applied to spathulenol, a sesquiterpene alcohol from peel oil of *Citrus junos* Tanaka.[8]

Experimental

N.m.r. spectra (400 MHz ^1H and 100 MHz ^{13}C) were recorded with a JEOL GX-400 spectrometer at 23 °C using $CDCl_3$ as solvent and Me_4Si as internal standard. Pulse sequences for INEPT, ^1H–^{13}C shift-correlated, ^1H shift-correlated, and n.O.e.-correlated 2D-n.m.r. were programmed and generated on a PG-200 pulse programmer. A 50 mg sample of spathulenol was used for the INEPT, ^1H–^{13}C shift-correlated, and n.O.e.-correlated 2D-n.m.r., and the difference n.O.e. A 5 mg sample was used for the ^1H shift-correlated 2D-n.m.r. All 2D-n.m.r. spectra were measured by using quadrature detection with the carrier frequency at the centre of the spectrum. For the measurement of ^1H–^{13}C shift-correlated 2D-n.m.r., spectral widths of 2 500 and 16 000 Hz were used for dimensions δ_1 and δ_2. The number of acquisition data points was 1 024, and digital resolution for the δ_2 axis was 31.3 Hz. Sixty-four scans were accumulated for each t_1 value, and 256 blocks were sampled. Subsequently, digital resolution for the δ_1 axis was 9.77 Hz. The total acquisition time was *ca.* 10 h. ^1H Shift-correlated 2D-n.m.r. was measured using the spectral width of 2 000 Hz for both dimensions δ_1 and δ_2. The number of acquisition data points was 1 024, and digital resolution for the δ_2 axis was 3.9 Hz. Thirty-two scans were accumulated for each t_1 value and 256 blocks were sampled. Thus the digital resolution for the δ_1 axis was 7.8 Hz. The total acquisition time was *ca.* 8 h. For the measurement of ^1H shift-correlated 2D-n.m.r. with delay time, the delay time was set at 300 ms. Other experimental conditions

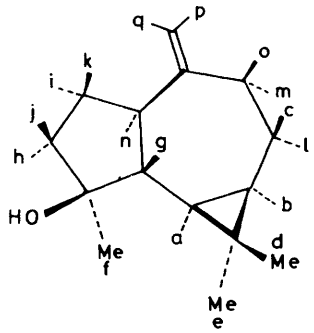

(1)

were the same for the ^1H shift-correlated 2D-n.m.r. The total acquisition time was *ca.* 10 h. The n.O.e.-correlated 2D-n.m.r. was measured with a mixing time of 1 000 ms. The spectral widths for both dimensions were 2 000 Hz. Sixteen scans were accumulated for each t_1 value and 256 blocks were sampled. The total acquisition time was *ca.* 10 h. For difference n.O.e. measurements, eight scans of on-resonance and off-resonance irradiation were accumulated alternately, and a total of 64 scans was sampled.

Results and Discussion

Spathulenol (**1**) is a tricyclic sesquiterpene alcohol.[8] Its 400 MHz ^1H and 100 MHz ^{13}C n.m.r. spectra are shown in Figure 1(a) and (b), respectively. The analysis of the ^1H n.m.r. spectrum is difficult owing to the close proximity of the resonances and also to the presence of a complicated network of spin–spin couplings. We therefore applied the strategy shown in Figure 2 for analysis of the n.m.r. spectra, starting with INEPT. Figure 3 shows INEPT[9,10] spectra of spathulenol with various delay times (Δ). At Δ = 1.8 ms all protonated carbon resonances give positive peaks [Figure 3(b)], and at Δ = 3.6 ms only CH carbon resonances are observed [Figure 3(c)]. When we set Δ at 5.6 ms, CH_2 carbon resonances gave negative peaks, while CH and CH_3 carbon resonances gave positive peaks [Figure 3(d)]. By comparison of INEPT spectra with different delay times, the ^{13}C resonances B, D, H, I, and L (not shown in Figure 3) were assigned to methylene carbons, and G, E, K, and J to methine carbons. Subsequently, A, C, and F were assigned to methyl carbons (Table 1). Thus, spathulenol was found to contain three methyl, five methylene, four methine, and three quaternary carbon atoms. In view of the chemical shifts of the ^{13}C

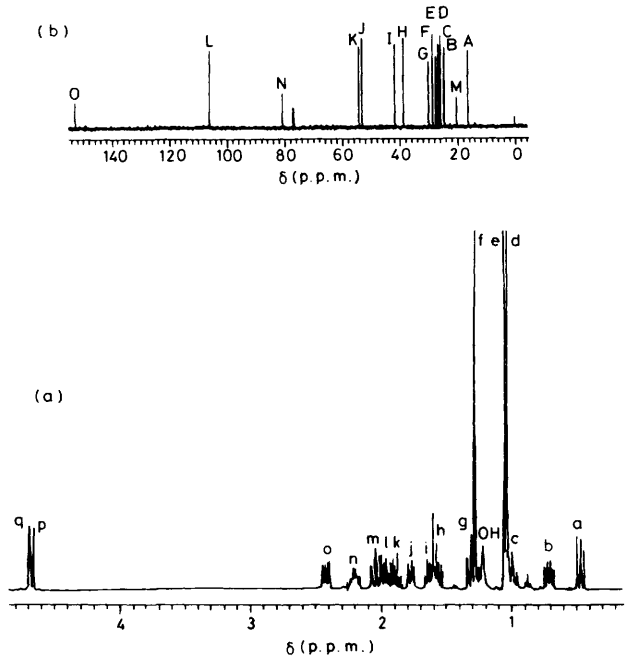

Figure 1. (a) 400 MHz ^1H n.m.r. spectrum and (b) 100 MHz ^{13}C n.m.r. spectrum of spathulenol

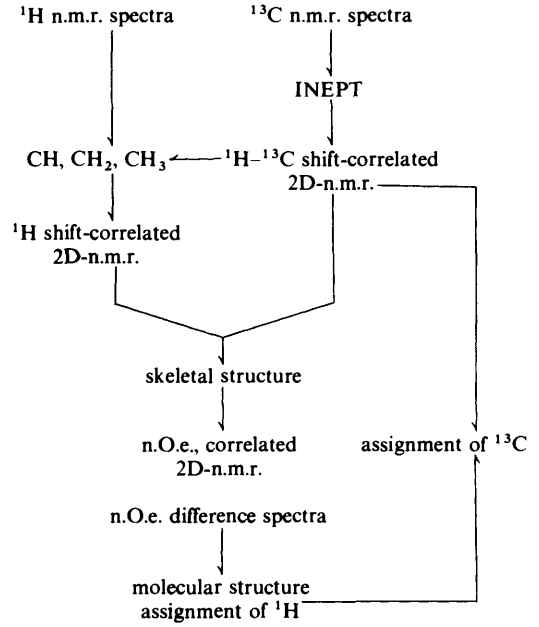

Figure 2. Strategy for the structure analysis of complex organic molecules by 2D-n.m.r.

resonances and the degree of unsaturation, spathulenol was thus shown to be a tricyclic sesquiterpene alcohol with $>C{=}CH_2$ and $\overset{|}{C}$–OH moieties.

The ^1H–^{13}C shift-correlated 2D-n.m.r.[11] was then studied, to identify the ^1H nuclei directly attached to the individual ^{13}C nuclei (Figure 4). From the correlated peaks, we were able to identify the pairs of ^{13}C and directly bonded ^1H nuclei as shown in Table 1. The proton resonances were developed in two dimensions according to the chemical shifts of the directly

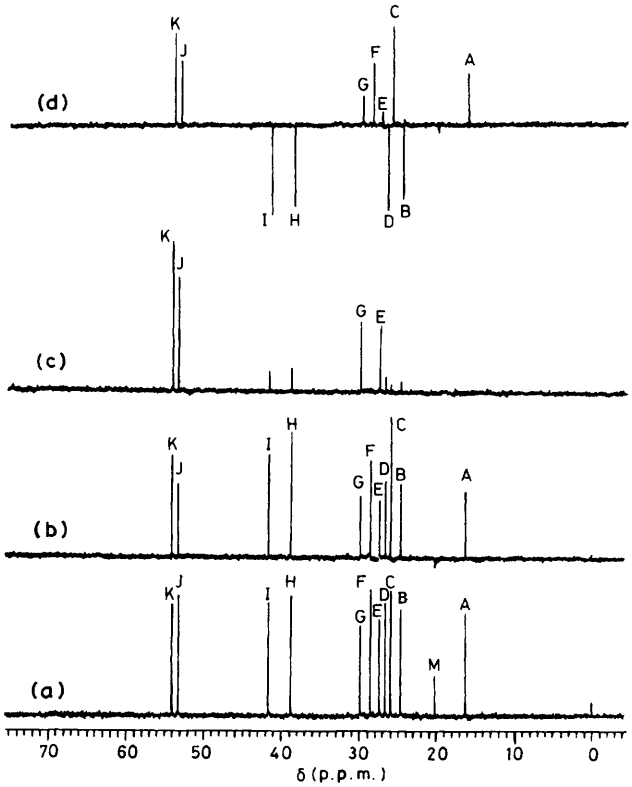

Figure 3. (a) Noise-decoupled ^{13}C n.m.r. spectrum of spathulenol. (b)–(d) INEPT spectra of spathulenol with various delay times: (b) 1.8 ms, (c) 3.6 ms, (d) 5.6 ms

Table 1. Assignment of ^{13}C resonances to CH_3, CH_2, CH, and quaternary carbon, and assignments of ^1H resonances directly bonded to specific carbon atoms

^{13}C	δ_c (p.p.m.)	Group	^1H	
A	16.33	CH_3	d	
B	24.77	CH_2	c,l	
C	26.06	CH_3	f	
D	26.72	CH_2	k,i	
E	27.46	CH	b	
F	28.66	CH_3	e	
G	29.77	CH	a	
H	38.88	CH_2	o,m	
I	41.75	CH_2	j,h	
J	53.43	CH	n	
K	54.29	CH	g	
L	106.27	CH_2	p,q	$>C{=}C^*H_2$
M	20.25	Quaternary		$-C^*-$
N	80.91	Quaternary		$-C^*-OH$
O	153.39	Quaternary		$>C^*{=}CH_2$

bonded ^{13}C resonances, so that the even overlapped resonances were well resolved. Furthermore, methylene protons with inequivalent chemical shifts were easily identified in the 2D spectrum. For example, methylene carbon atoms I and H were found to bear protons j,h and o,m, respectively. These points show the significant advantages of ^1H–^{13}C shift-correlated 2D-n.m.r. over conventional selective decoupling methods.

The connectivity of the carbon atoms was then determined through analysis of the network of ^1H spin–spin couplings using

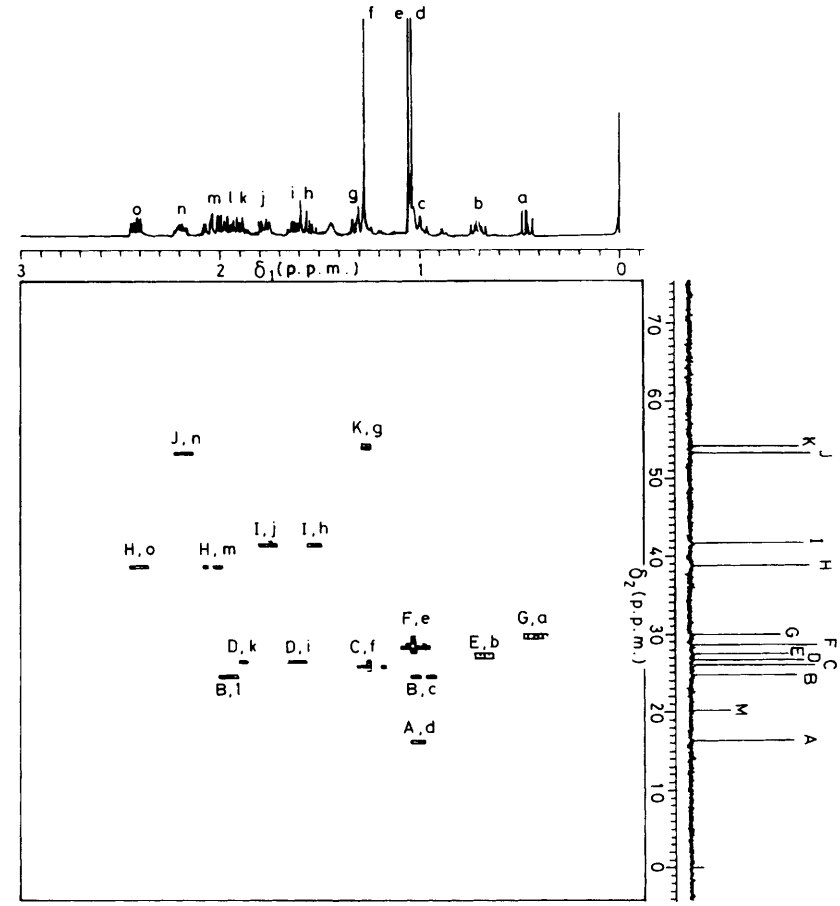

Figure 4. ^{1}H–^{13}C Shift-correlated 2D-n.m.r. spectrum of spathulenol

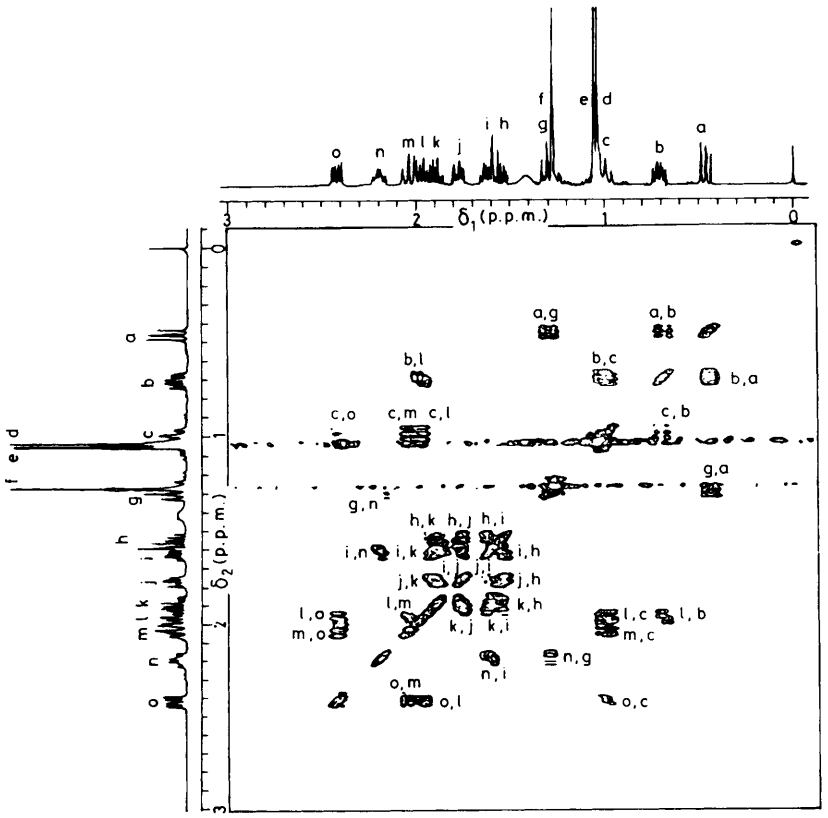

Figure 5. ^{1}H Shift-correlated 2D-n.m.r. spectrum of spathulenol without delay time

^{1}H shift-correlated 2D-n.m.r.[12] Figure 5 shows the ^{1}H shift-correlated spectrum observed by using the pulse sequence 90°–t_1–45°–t_2.[13] In the present study, we used a 45° rather than a 90° pulse as mixing pulse. The intensity of the cross peaks relative to the diagonal peaks is enhanced, so that the cross peaks located close to the diagonal peaks (such as i,h and k,j) can be easily observed. Figure 5 shows the cross peaks due to geminal and vicinal couplings with more than *ca.* 3 Hz. From the cross peaks due to vicinal couplings, the connectivities of carbon atoms in spathulenol could be determined as shown in Figure 6. However, at this stage, the connectivities of the quaternary carbon nuclei could not be determined (broken lines in Figure 6).

In order to locate the quaternary carbon nuclei, ^{1}H shift-correlated 2D-n.m.r. with delay time was measured. Figure 7 shows the spectrum observed by using the 90°–Δ–t_1–45°–Δ–t_2 sequence,[13] when Δ (delay time) was set to 300 ms. The cross peaks due to small couplings (less than *ca.* 1 Hz) are enhanced, while those due to large couplings (more than *ca.* 3 Hz) are suppressed (Figure 7). For example, the cross peaks a,e and b,e are due to the long-range couplings between the methyl proton e and the methine protons a and b, respectively. Thus, the connectivity of the quaternary carbon M bearing methyl group e to the methine carbon nuclei G and E was established. In the same manner, the presence of the cross peaks n,q and m,p shows the connectivity of the quaternary carbon O to the methine carbon J and the methylene carbon H. The cross peaks h,f and j,g also show the connectivity of the quaternary carbon N to the methylene carbon I and the methine carbon K. Thus, the skeletal structure of spathulenol was determined as shown in Figure 6. The final stage was to determine the three-dimensional structure of spathulenol using n.O.e.-correlated 2D-n.m.r.[14] and n.O.e. difference spectra,[15] based on the skeletal structure (Figure 6). The n.O.e.-correlated spectrum in a contour plot is shown in Figure 8; the pulse sequence 90°–t_1–90°–τ_m–90°–t_2 was used. In the present study, we used 1 000 ms for τ_m, since the n.O.e. is small and its build-up rate is relatively low for small molecules.[14] A long mixing time also removes cross peaks due to zero quantum coherence. The cross peaks o,m, l,c, k,i, and j,h are due to the methylene proton pairs and are trivial. There are many cross peaks in the spectrum, which is useful for elucidating the three-dimensional structure. For example, the cross peaks a,e, a,f, and a,b show the close proximity of the protons e, f, and b to the methine proton a, indicating that these protons stick out to one side of the molecule. The cross peak g,d also shows the close proximity of the methine proton g and the methyl proton d, indicating that these protons stick out to the other side of the molecule. However, in the contour plot, the cross peaks below the threshold are not observed; it is often useful to detect small n.O.e. effects by using the conventional 1D n.O.e. difference method. Figure 9 shows the n.O.e. difference spectra

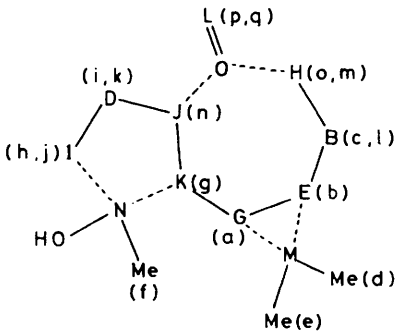

Figure 6. Skeletal structure of spathulenol

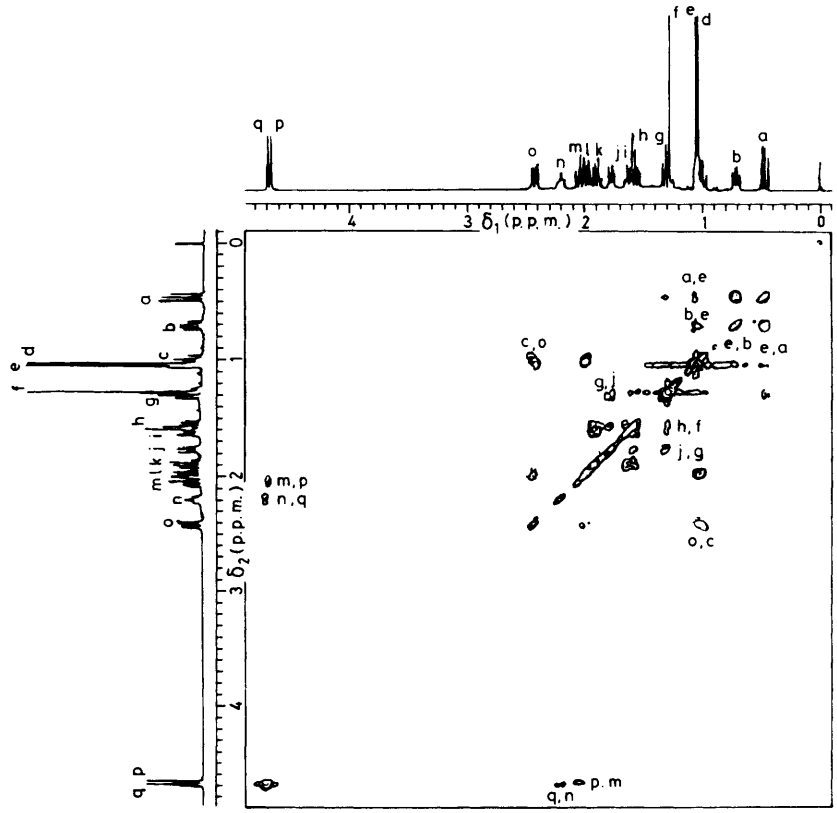

Figure 7. ^{1}H Shift-correlated 2D-n.m.r. spectrum of spathulenol with delay time of 300 ms

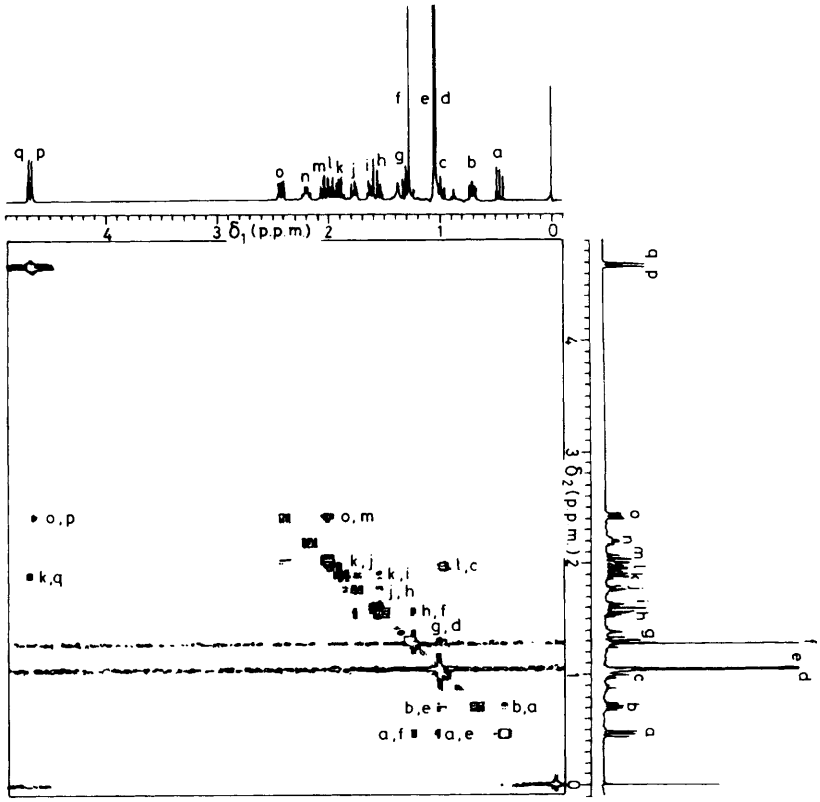

Figure 8. N.O.e.-correlated 2D-n.m.r. spectrum of spathulenol with mixing time of 1000 ms

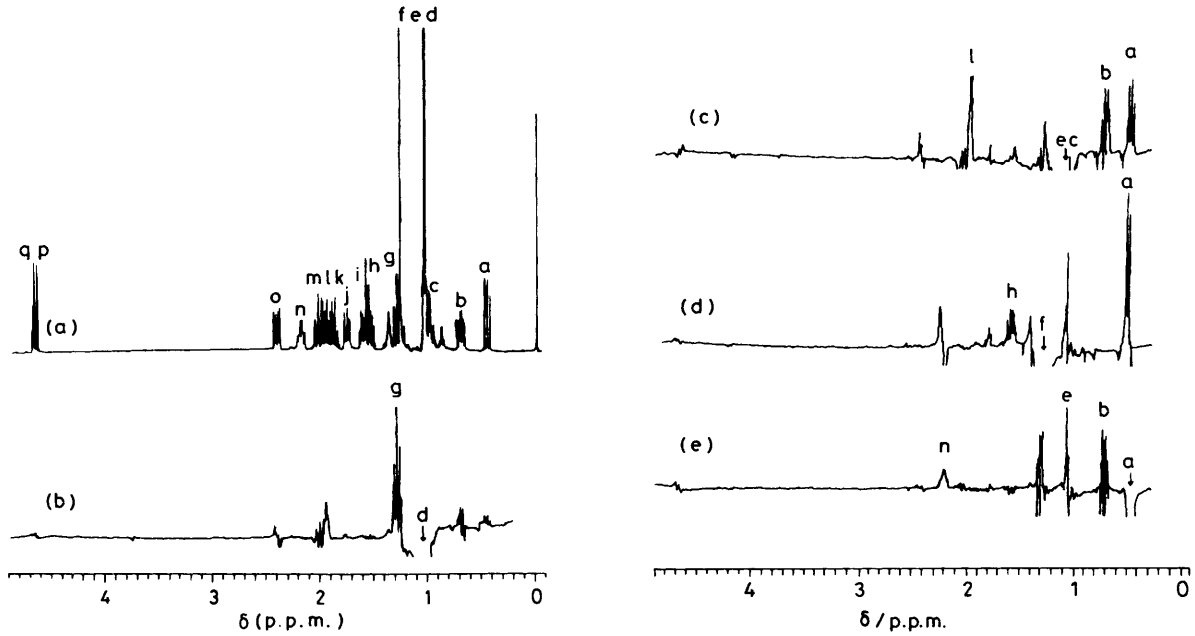

Figure 9. N.O.e. difference spectra of spathulenol: (a) normal spectrum; (b)—(e) irradiation at resonances d, e, f, and a

of spathulenol (difference between on-resonance and off-resonance irradiation). On irradiation at the methyl proton resonance d, n.O.e. was observed on the methine proton resonance g [Figure 9(b)]. When the methyl proton resonance e was irradiated, n.O.e. was observed on the methine proton resonances a and b [Figure 9(c)]. Moreover, when the methyl proton resonance f was irradiated, n.O.e. was observed on the methine proton resonance a [Figure 9(d)]. These results are in good agreement with those observed by n.O.e.-correlated 2D-n.m.r. In addition, on irradiation at the methine proton resonance a, we observed n.O.e. on the methine proton resonance n, indicating that the methine protons a and n are located in close proximity [Figure 9(e)]. Thus, the configuration at the junction between the five-and seven-membered rings was found to be *trans*. From the n.O.e. measurements, the configuration and conformation of spathulenol was determined as

Table 2. ^{1}H Chemical shifts of spathulenol; correlation from ^{1}H shift-correlated and n.O.e.-correlated 2D-n.m.r.

^{1}H	δ_H (p.p.m.)	^{1}H Shift-correlated	N.O.e.-correlated	
a	0.463	b,g	b,e,f,n	CH
b	0.707	a,c,l	a,e	CH
c	1.010	b,m,l,o	l	c,l CH_2
d	1.038		g	CH_3
e	1.053		a,b	CH_3
f	1.278		a,e,h	CH_3
g	1.305	a,n	d	CH
h	1.540	i,j,k	f,j	h,j CH_2
i	1.640	j,k,h,n	k	k,i CH_2
j	1.771	h,k,i	h,k	h,j CH_2
k	1.909	i,j,h,n	i,j	k,i CH_2
l	1.960	b,c,o,m	c	c,l CH_2
m	2.037	c,o,l	o	o,m CH_2
n	2.196	g,i,k	a	CH
o	2.418	c,l,m	m	o,m CH_2
p	4.662	m,q	o	p,q CH_2
q	4.688	n,p	k	p,q CH_2

shown in (**1**). At the same time, the assignments of all the carbon and proton resonances were accomplished (Tables 1 and 2).

Conclusion

The present strategy takes advantage of high resolving power of ^{13}C n.m.r. in order to correlate pairs of the directly bonded ^{1}H and ^{13}C nuclei. Thus we can identify ^{1}H resonances even from the crowded region of the ^{1}H n.m.r. spectrum. In this sense, ^{1}H–^{13}C shift-correlated 2D-n.m.r. is a key step in the present strategy. However, the sensitivity of ^{1}H–^{13}C shift-correlated 2D-n.m.r. is a severe problem for its application to structural analysis. The minimum amount of sample was found to be *ca.* 10 mg for a sesquiterpene. This may be further reduced by improving the sensitivity by probe design, sampling techniques, or pulse techniques. In fact we applied ^{1}H homonuclear decoupling during evolution time, so that the sensitivity was improved by a factor of more than two. The present strategy will be particularly appropriate for the structural analysis of complicated organic molecules available only in small quantities.

Acknowledgements

We are grateful to Professor R. J. P. Williams (Oxford) for discussions.

References

1 R. Freeman and G. A. Morris, *Bull. Magn. Reson.*, 1979, **1**, 5.
2 R. Freeman, *Proc. R. Soc. London, Ser. A*, 1980, **373**, 149.
3 K. Nagayama, *Adv. Biophys.*, 1981, **14**, 139.
4 A. Bax, 'Two Dimensional Nuclear Magnetic Resonance in Liquids,' Reidel Dordrecht, 1982.
5 A. Bax, R. Freeman, and T. A. Frenkiel, *J. Am. Chem. Soc.*, 1981, **103**, 2102.
6 A. Bax, R. Freeman, and S. P. Kempsell, *J. Am. Chem. Soc.*, 1980, **102**, 4849.
7 A. Bax, R. Freeman, and S. P. Kempsell, *J. Magn. Reson.*, 1980, **41**, 349.
8 N. Shinoda, M. Shiga, and K. Nishimura, *Agric. Biol. Chem.*, 1970, **34**, 234.
9 G. A. Morris and R. Freeman, *J. Am. Chem. Soc.*, 1979, **101**, 760.
10 D. M. Doddrell and D. T. Pegg, *J. Am. Chem. Soc.*, 1980, **102**, 6388.
11 R. Freeman and G. A. Morris, *J. Chem. Soc., Chem. Commun.*, 1978, 64.
12 W. P. Aue, E. Bartholdi, and R. R. Ernst, *J. Chem. Phys.*, 1976, **64**, 2229.
13 A. Bax and R. Freeman, *J. Magn. Reson.*, 1981, **44**, 542.
14 S. Macura and R. R. Ernst, *Mol. Phys.*, 1980, **41**, 95.
15 J. K. M. Sanders and J. D. Mersh, *Prog. Nucl. Magn. Reson. Spectrosc.*, 1982, **15**, 353.

Received 18*th February* 1985; *Paper* 5/280